

Brief paper

Manipulator motion control in operational space using joint velocity inner loops[☆]

Rafael Kelly^{a,*}, Javier Moreno^b

^a*Telematica, CICESE, Apdo. Postal 2615, Adm. 1, Ensenada, BC 22800, Mexico*

^b*Systems and Control, Department of Electrical Engineering and Computer Science, B28 Université de Liège, B-4000 Liège Sart, Tilman, Belgium*

Received 5 December 2003; received in revised form 14 September 2004; accepted 14 March 2005

Abstract

This paper addresses the operational space motion control—trajectory tracking—of robot manipulators endowed with joint velocity feedback inner loops. A general structure for model-based joint velocity controllers is proposed for the inner loop. The required joint velocity reference is provided by an outer loop inspired from the robot kinematic control approach. It is shown that above two-loops control schemes lead to a nice cascade structure for the corresponding closed-loop systems. A stability result adapted for analysis of this particular kind of systems is developed in the paper; sufficient conditions for global exponential stability of this class of cascade systems are obtained. The effectiveness of the proposed control approach is evaluated on a direct-drive mechanical arm, and compared with a typical control strategy based on inverse kinematics resolution for computation of the desired motion in joint space, and the use of the computed-torque technique. The experimental evidences show better performance of the proposed two-loops controller.

© 2005 Published by Elsevier Ltd.

Keywords: Manipulator control; Cascade systems stability; Exponential stability; Operational space; Direct-drive robot

1. Introduction

Robot manipulators desired motions are typically specified in terms of desired trajectories of the end-effector pose—position and orientation—in operational space (Canudas, Siciliano, & Bastin, 1996; Sciavicco & Siciliano, 2000). The motion control problem in operational space concerns the computation of suitable joint torques in such a way that the manipulator end-effector pose matches asymptotically the desired pose trajectory.

The actual situation of many industrial robots is that the control of each electro-mechanical axis is carried out using inner joint velocity loops in addition to outer position loops

(Corke, 1994; Nilsson, 1996). This practical fact motivates the investigation and analysis of control schemes based on joint velocity feedback inner loop for achieving operational space motion control.

Although the practice of motion control in operational space of robot manipulators driven by low-level joint velocity inner loops is well established, in contrast few efforts about analysis of control of mechanical systems in operational space considering joint velocity feedback inner loops have been reported in the literature. One exception is the work of Aicardi, Caili, Cannata, and Casalino (1995) where the inverse differential kinematics is utilized for joint velocity resolution as outer loop, and a joint velocity controller motivated from the computed-torque control (Spong & Vidyasagar, 1989) is evoked as inner loop. Notwithstanding, the joint velocity controller does not consider joint velocity error integral action, which usually improves the robustness of the system.

This paper studies motion control systems for manipulators in operational space having a two-loops feedback

[☆] This paper was not presented at any IFAC meeting. This paper was recommended for publication in revised form by Associate Editor G. Obinata under the direction of Editor M. Araki. Work partially supported by CONACyT, and CYTED.

* Corresponding author. Fax: +52 646 1 75 05 37.

E-mail address: rkelly@cicese.mx (R. Kelly).

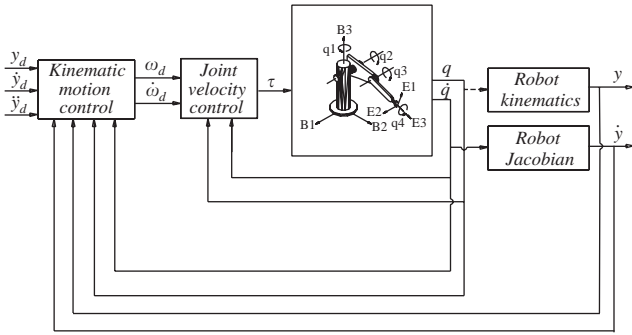


Fig. 1. Block diagram of the control scheme based on velocity feedback inner loops.

structure, namely, a joint velocity inner loop, and an operational space kinematic control outer loop, see Fig. 1. One important conclusion of this paper is the recognition that the overall closed-loop dynamics can be seen as a cascade system whose stability may be analysed by invoking a number of general stability tools available in the literature. Cascade system stability theory has been successfully used in control problems such as synchronization of two pendula, tracking control of robots with AC drives, set-point stabilization of a turbo-charged diesel engine (Panteley, Loria, & Sokolov, 1999), and dynamic positioning of ships using only position measurements (Loria, Fossen, & Panteley, 2000).

Sufficient conditions for asymptotic stability of nonlinear autonomous systems in cascade form have been well studied, see for instance Sepulchre, Janković, and Kokotović (1997), Isidori (1999), and references therein. With respect to nonlinear nonautonomous systems in cascade structure, sufficient conditions for Global Uniform Asymptotic Stability (GUAS) can be consulted for instance in Khalil (1996), and Panteley and Loria (1998). In the latter work, absolute integrability on the solution of the independent system is assumed. Later, Panteley et al. (1999) developed a similar theory but assuming that the origin of the independent system is Globally Exponentially Stable¹ (GES). Inspired by Khalil (1996), Panteley and Loria (1998), and Panteley et al. (1999), this paper presents simple conditions for GES of the particular cascade structure derived from motion control systems in operational space of manipulators.

The main contribution of this paper is the introduction and analysis of a class of operational space trajectory tracking controllers based on two-loops of feedback. More specifically, the outer loop is given by a kinematic control for joint velocity resolution as operational space, and the inner loop is formed by exponentially stable joint velocity controllers. Two model-based joint velocity controllers are proposed for being used in the inner control loop. The first one holds an inverse dynamics structure (Spong & Vidyasagar, 1989), while the second one resembles the PD control with com-

pensation structure (Slotine & Li, 1991). One advantage of the proposed controllers is that the specified motions can be executed directly in the operational space, and off-line computation of the inverse kinematics is not required. As previously pointed out, the closed-loop dynamics resulting of the kinematic control plus the joint velocity controllers have a cascade system form. For the sake of completeness, this paper presents sufficient conditions for GES of the closed-loop systems. They are well adapted conditions than those obtained from standard results extracted from the literature because the particular cascade structure studied.

The paper is supported with results of the experimental evaluation carried out on a two degrees-of-freedom direct-drive arm. In conclusion, it is demonstrated that: (1) the practical viability of the proposed approach to operational space robot control, and (2) the superiority of the proposed controllers with respect to a joint space-based controller.

This paper is organized as follows. Section 2 concerns the robot dynamics and control problem formulation. Section 3 is devoted to cascade systems stability. In Section 4 a class of motion control systems in operational space based on velocity feedback inner loops is introduced. In Section 5 two model-based joint velocity controllers that work together with kinematic control are proposed. Experimental results are described in Section 6, and some concluding remarks are given in Section 7.

Throughout this paper the following notation will be adopted. $\lambda_m\{A\}$ and $\lambda_M\{A\}$ denote the minimum and maximum eigenvalues of a symmetric positive definite matrix $A(x) \in \mathbb{R}^{n \times n}$ for all $x \in \mathbb{R}^n$, respectively. $\|x\| = \sqrt{x^T x}$ stands for the norm of vector $x \in \mathbb{R}^n$. $\|B(x)\| = \sqrt{\lambda_M\{B(x)^T B(x)\}}$ stands for the induced norm of a matrix $B(x) \in \mathbb{R}^{m \times n}$ for all $x \in \mathbb{R}^n$.

2. Robot dynamics and control aim

In absence of friction and other disturbance the dynamics of a serial n -link robot manipulator can be written as (Spong & Vidyasagar, 1989):

$$M(q)\ddot{q} + C(q, \dot{q})\dot{q} + g(q) = \tau, \quad (1)$$

where $q \in \mathbb{R}^n$ is the joint position vector, \dot{q} denotes the joint velocity, $\tau \in \mathbb{R}^n$ is the applied torque input vector, $M(q) \in \mathbb{R}^{n \times n}$ is the symmetric positive definite manipulator inertia matrix, $C(q, \dot{q})\dot{q} \in \mathbb{R}^n$ is the vector of centripetal and Coriolis torques, and $g(q) \in \mathbb{R}^n$ stands for the vector of gravitational torques due to the gravity.

The matrix $C(q, \dot{q})$ —defined by using Christoffel symbols—and the time derivative of the inertia matrix $\dot{M}(q)$ satisfy (Canudas et al., 1996)

$$x^T \left[\frac{1}{2} \dot{M}(q) - C(q, \dot{q}) \right] x = 0 \quad \forall x, q, \dot{q} \in \mathbb{R}^n. \quad (2)$$

¹ In this paper the abbreviation GES will be used for both “Globally Exponentially Stable” and “Global Exponential Stability.”

Let $\mathbf{h}(\mathbf{q}) : \mathbb{R}^n \rightarrow \mathbb{R}^m$ be the robot direct kinematics ($n \geq m$); then the pose—position and orientation— $\mathbf{y} \in \mathbb{R}^m$ of the end-effector is given by

$$\mathbf{y} = \mathbf{h}(\mathbf{q}). \tag{3}$$

The time derivative of the direct kinematic model (3) yields the differential kinematic model

$$\dot{\mathbf{y}} = \frac{d}{dt} \mathbf{h}(\mathbf{q}) = \frac{\partial \mathbf{h}}{\partial \mathbf{q}} \dot{\mathbf{q}} = \mathbf{J}(\mathbf{q}) \dot{\mathbf{q}}, \tag{4}$$

where $\mathbf{J}(\mathbf{q})$ is the so-called analytical Jacobian matrix (Canudas et al., 1996). In general this matrix loses rank at singular configurations. When computation of the inverse or pseudoinverse of the Jacobian is required, a damped least-squares inverse can be adopted to gain robustness in the neighborhood of the kinematic singularities (Wampler & Leifer, 1988), or a pseudoinverse in conjunction with a suitable term in the null space of the Jacobian describing the internal motion of the manipulator (Hsu, Hauser, & Sastry, 1989) can be utilized. Since the focus of the present work is on problems related to cascade representation of feedback loops, without loss of generality, the Jacobian $\mathbf{J}(\mathbf{q})$ is assumed to be full-rank (rank = m) and bounded by $k_J > 0$, i.e.

$$\|\mathbf{J}(\mathbf{q})\| \leq k_J \quad \forall \mathbf{q} \in \mathbb{R}^n. \tag{5}$$

Once the motion specification is given in terms of the desired trajectory $\mathbf{y}_d(t)$ in the operational space, then the motion control objective in operational space is to achieve:

$$\lim_{t \rightarrow \infty} \tilde{\mathbf{y}}(t) = \mathbf{0}, \tag{6}$$

where $\tilde{\mathbf{y}}(t) = \mathbf{y}_d(t) - \mathbf{y}(t)$ denotes the operational space pose error.

3. GES of cascade systems

This Section is devoted to present the application of results introduced in Khalil (1996), Panteley and Loria (1998), and Panteley et al. (1999), about stability of interconnected and cascade systems to a particular kind of cascade system useful for the analysis of motion control of manipulators having an underlying two-loops structure. Following the notation in Panteley and Loria (1998), Panteley et al. (1999), consider the system

$$\Sigma_1: \dot{\mathbf{x}}_1 = \mathbf{f}_1(t, \mathbf{x}_1) + \mathbf{g}(t, \mathbf{x}) \mathbf{x}_2, \tag{7}$$

$$\Sigma_2: \dot{\mathbf{x}}_2 = \mathbf{f}_2(t, \mathbf{x}_2), \tag{8}$$

where $\mathbf{x}_1 \in \mathbb{R}^{n_1}$, $\mathbf{x}_2 \in \mathbb{R}^{n_2}$ and $\mathbf{x} = [\mathbf{x}_1^T \ \mathbf{x}_2^T]^T$. Suppose that $\mathbf{f}_1(t, \mathbf{x}_1)$, $\mathbf{f}_2(t, \mathbf{x}_2)$ and $\mathbf{g}(t, \mathbf{x})$ are smooth enough to ensure global existence and uniqueness of the solution for all initial

conditions, and that

$$\mathbf{f}_1(t, \mathbf{0}) = \mathbf{0},$$

$$\mathbf{f}_2(t, \mathbf{0}) = \mathbf{0},$$

for all $t \geq 0$, so that the origin $\mathbf{x} = \mathbf{0} \in \mathbb{R}^{n_1+n_2}$ is an equilibrium point of system (7) and (8).

Ignoring the disturbing term $\mathbf{g}(t, \mathbf{x})$, system (7) and (8) becomes the decoupled system

$$\Sigma'_1: \dot{\mathbf{x}}_1 = \mathbf{f}_1(t, \mathbf{x}_1), \tag{9}$$

$$\Sigma'_2: \dot{\mathbf{x}}_2 = \mathbf{f}_2(t, \mathbf{x}_2). \tag{10}$$

We wish to extract conditions on the “perturbation” $\mathbf{g}(t, \mathbf{x})$ such that GES of the system $\Sigma'_1 - \Sigma'_2$ implies GES of the original system $\Sigma_1 - \Sigma_2$. To this end, a number of assumptions shall be needed. Suppose that there exist Lyapunov functions $V_1(t, \mathbf{x}_1)$ and $V_2(t, \mathbf{x}_2)$ for Σ'_1 and Σ'_2 , respectively, such that

$$\begin{aligned} c_1 \|\mathbf{x}_1\|^2 &\leq V_1(t, \mathbf{x}_1) \leq c_2 \|\mathbf{x}_1\|^2, \\ d_1 \|\mathbf{x}_2\|^2 &\leq V_2(t, \mathbf{x}_2) \leq d_2 \|\mathbf{x}_2\|^2 \end{aligned} \tag{11}$$

for all $t \geq 0$, $\mathbf{x}_1 \in \mathbb{R}^{n_1}$, $\mathbf{x}_2 \in \mathbb{R}^{n_2}$, and some positive constants c_1 , c_2 , d_1 , and d_2 . Moreover, suppose that there exist positive constants c_3 and d_3 satisfying

$$\begin{aligned} \left\| \frac{\partial V_1(t, \mathbf{x}_1)}{\partial \mathbf{x}_1} \right\| &\leq c_3 \|\mathbf{x}_1\|, \\ \left\| \frac{\partial V_2(t, \mathbf{x}_2)}{\partial \mathbf{x}_2} \right\| &\leq d_3 \|\mathbf{x}_2\| \end{aligned} \tag{12}$$

for all $t \geq 0$, $\mathbf{x}_1 \in \mathbb{R}^{n_1}$, $\mathbf{x}_2 \in \mathbb{R}^{n_2}$.

Finally, suppose that the derivative of these Lyapunov functions along the system trajectories (9) and (10) satisfy

$$\begin{aligned} \dot{V}_1(t, \mathbf{x}_1) &= \frac{\partial V_1}{\partial t} + \frac{\partial V_1}{\partial \mathbf{x}_1} \mathbf{f}_1 \leq -c_4 \|\mathbf{x}_1\|^2, \\ \dot{V}_2(t, \mathbf{x}_2) &= \frac{\partial V_2}{\partial t} + \frac{\partial V_2}{\partial \mathbf{x}_2} \mathbf{f}_2 \leq -d_4 \|\mathbf{x}_2\|^2 \end{aligned} \tag{13}$$

for all $t \geq 0$, $\mathbf{x}_1 \in \mathbb{R}^{n_1}$, $\mathbf{x}_2 \in \mathbb{R}^{n_2}$, and some positive constants c_4 , and d_4 .

Above requirements on $V_1(t, \mathbf{x}_1)$ and $V_2(t, \mathbf{x}_2)$ are enough to establish GES of system Σ'_1 and Σ'_2 (Vidyasagar, 1993; Khalil, 1996).

On the other hand, suppose that the perturbation $\mathbf{g}(t, \mathbf{x})$ satisfy the inequality:

$$\|\mathbf{g}(t, \mathbf{x}) \mathbf{x}_2\| \leq \psi \|\mathbf{x}_2\| \tag{14}$$

for some strictly positive constant ψ , and for all $t \geq 0$, $\mathbf{x}_1 \in \mathbb{R}^{n_1}$, $\mathbf{x}_2 \in \mathbb{R}^{n_2}$.

We are ready to present the following:

Proposition 1. *Suppose that there exist Lyapunov functions $V_1(t, \mathbf{x}_1)$ and $V_2(t, \mathbf{x}_2)$ for decoupled system (9), (10) satisfying (11)–(13). Moreover, assume that the disturbing term*

$g(t, \mathbf{x})\mathbf{x}_2$ satisfies (14). Then, the equilibrium point $\mathbf{x} = \mathbf{0}$ of the cascade system (7) and (8) is GES.

Proof. We propose the following Lyapunov function candidate for the cascaded system (7) and (8):

$$V(t, \mathbf{x}) = \delta V_1(t, \mathbf{x}_1) + V_2(t, \mathbf{x}_2), \tag{15}$$

where δ is a positive constant such that

$$\delta < \frac{4c_4d_4}{c_3^2\psi^2}. \tag{16}$$

In view of assumption (11) on $V_1(t, \mathbf{x}_1)$ and $V_2(t, \mathbf{x}_2)$, it turns out that

$$\min\{\delta c_1, d_1\}\|\mathbf{x}\|^2 \leq V(t, \mathbf{x}) \leq \max\{\delta c_2, d_2\}\|\mathbf{x}\|^2$$

for all $t \geq 0$, and $\mathbf{x} \in \mathbb{R}^{n_1+n_2}$.

On the other hand, invoking inequalities (12), it can be shown that

$$\left\| \frac{\partial V(t, \mathbf{x})}{\partial \mathbf{x}} \right\| \leq \max\{\delta c_3, d_3\}\|\mathbf{x}\|$$

for all $t \geq 0$, and $\mathbf{x} \in \mathbb{R}^{n_1+n_2}$.

The time derivative of $V(t, \mathbf{x})$ along of the system trajectories (7) and (8) is given by

$$\begin{aligned} \dot{V}(t, \mathbf{x}) = & \delta \left[\frac{\partial V_1}{\partial t} + \frac{\partial V_1}{\partial \mathbf{x}_1} \mathbf{f}_1(t, \mathbf{x}_1) + \frac{\partial V_1}{\partial \mathbf{x}_1} \mathbf{g}(t, \mathbf{x})\mathbf{x}_2 \right] \\ & + \frac{\partial V_2}{\partial t} + \frac{\partial V_2}{\partial \mathbf{x}_2} \mathbf{f}_2(t, \mathbf{x}_2). \end{aligned} \tag{17}$$

In virtue of (12)–(14), the following upper bound on $\dot{V}(t, \mathbf{x})$ is obtained

$$\dot{V}(t, \mathbf{x}) \leq - \underbrace{\begin{bmatrix} \|\mathbf{x}_1\| \\ \|\mathbf{x}_2\| \end{bmatrix}^T \begin{bmatrix} \delta c_4 & -\frac{1}{2}\delta c_3\psi \\ -\frac{1}{2}\delta c_3\psi & d_4 \end{bmatrix} \begin{bmatrix} \|\mathbf{x}_1\| \\ \|\mathbf{x}_2\| \end{bmatrix}}_Q. \tag{18}$$

It is worth noticing that the symmetric matrix Q is positive definite because δ satisfies inequality (16); thus $\lambda_m\{Q\} > 0$. This allows to write

$$\dot{V}(t, \mathbf{x}) \leq -\lambda_m\{Q\}\|\mathbf{x}\|^2$$

for all $t \geq 0$, and $\mathbf{x} \in \mathbb{R}^{n_1+n_2}$.

Therefore, according to the Lyapunov direct method (Vidyasagar, 1993; Khalil, 1996), the conclusion of GES of the state space origin of the cascade system (7) and (8) is established, hence

$$\lim_{t \rightarrow \infty} \begin{bmatrix} \mathbf{x}_1(t) \\ \mathbf{x}_2(t) \end{bmatrix} = \mathbf{0}$$

exponentially. \square

4. Kinematic control plus joint velocity inner loop

Kinematic control considers the differential kinematics (4) as the robot model; thus the joint velocity $\dot{\mathbf{q}}$ is treated as the input of the robot, and the pose \mathbf{y} is kept as its output.

4.1. Kinematic control outer loop

Let us consider the resolved motion rate control (Whitney, 1969) to compute the desired *inner* joint velocity ω_d as

$$\omega_d = J(\mathbf{q})^\dagger [\dot{\mathbf{y}}_d + K\tilde{\mathbf{y}}], \tag{19}$$

where $K \in \mathbb{R}^{n \times n}$ is a symmetric positive definite matrix, and

$$J(\mathbf{q})^\dagger = J(\mathbf{q})^T [J(\mathbf{q})J(\mathbf{q})^T]^{-1}$$

is the Jacobian right pseudoinverse (Canudas et al., 1996). Under the assumption of perfect velocity tracking, i.e., $\dot{\mathbf{q}} \equiv \omega_d$, by substituting the desired joint velocity (19) in the differential kinematics (4) we have

$$\dot{\tilde{\mathbf{y}}} = -K\tilde{\mathbf{y}}. \tag{20}$$

Since K is a symmetric positive definite matrix, then we have that $\tilde{\mathbf{y}}(t) \rightarrow \mathbf{0}$ as $t \rightarrow \infty$. This means that the motion control objective in operational space is attained as far as the manipulators are equipped with perfect joint velocity controllers.

However, in practice the joint velocity controllers cannot achieve instantaneous perfect tracking of the requested joint velocity; therefore, assumption of ideal velocity tracking should be relaxed.

Let us define the joint velocity error as

$$\tilde{\omega} = \omega_d - \dot{\mathbf{q}}. \tag{21}$$

Hence, a system Σ_1 can be obtained from the differential kinematic (4), the control law (19), and the definition of the joint velocity error (21) as

$$\Sigma_1: \frac{d}{dt}\tilde{\mathbf{y}} = -K\tilde{\mathbf{y}} + J(\mathbf{q})\tilde{\omega}. \tag{22}$$

Practical implementation of kinematic control (19) involves the design of a suitable joint velocity controller (inner loop) to achieve asymptotic joint velocity tracking, i.e.

$$\lim_{t \rightarrow \infty} \tilde{\omega}(t) = \lim_{t \rightarrow \infty} [\omega_d(t) - \dot{\mathbf{q}}(t)] = \mathbf{0}.$$

4.2. Joint velocity inner loop

The class of velocity controllers discussed in this paper has underlying proportional-integral action driven by the joint velocity error $\tilde{\omega}$. A quite general structure for such joint

velocity control systems is

$$\tau = M(\mathbf{q})[\dot{\omega}_d + \xi(\mathbf{q}, \dot{\mathbf{q}}, \mathbf{z}, \tilde{\omega})] + C(\mathbf{q}, \dot{\mathbf{q}})\dot{\mathbf{q}} + \mathbf{g}(\mathbf{q}), \quad (23)$$

$$\dot{\mathbf{z}} = \tilde{\omega}, \quad (24)$$

where $\xi(\mathbf{q}, \dot{\mathbf{q}}, \mathbf{z}, \tilde{\omega}) \in \mathbb{R}^n$ is a continuous function such that $\xi(\mathbf{q}, \dot{\mathbf{q}}, \mathbf{0}, \mathbf{0}) = \mathbf{0}$. It shall be shown later that $\xi(\mathbf{q}, \dot{\mathbf{q}}, \mathbf{z}, \tilde{\omega})$ can be chosen in such a way that the joint velocity controller (23) and (24) have a model-based structure like the inverse dynamics, and the PI control with compensation. The state \mathbf{z} denotes the integral of the joint velocity error $\tilde{\omega}$, and

$$\dot{\omega}_d = \left[\frac{d}{dt} J(\mathbf{q})^\dagger \right] [\dot{\mathbf{y}}_d + K\tilde{\mathbf{y}}] + J(\mathbf{q})^\dagger [\ddot{\mathbf{y}}_d + K\dot{\tilde{\mathbf{y}}}] \quad (25)$$

corresponds to the desired joint acceleration obtained by differentiating (19).

It is worth noticing that by substituting the general structure of the joint velocity control (23), (24) into the robot dynamics (1) produces

$$\Sigma_2: \frac{d}{dt} \begin{bmatrix} \mathbf{z} \\ \tilde{\omega} \end{bmatrix} = \begin{bmatrix} \tilde{\omega} \\ -\xi(\mathbf{q}, \dot{\mathbf{q}}, \mathbf{z}, \tilde{\omega}) \end{bmatrix}. \quad (26)$$

4.3. Two-loop control system dynamics

Systems Σ_1 and Σ_2 , expressed by (22) and (26), represent the closed-loop dynamics of the two-loops control system composed by the kinematic control (19) (outer loop) together with the joint velocity control (23) and (24) (inner loop). It is clear that the closed-loop dynamics has a cascade structure, since the signal $\tilde{\omega}$ disturbs the dynamics of $\tilde{\mathbf{y}}$ in Eq. (22).

By neglecting the disturbing term $J(\mathbf{q})\tilde{\omega}$ in (22), it is straightforward to obtain the decoupled systems:

$$\Sigma_1': \frac{d}{dt} \mathbf{y} = -K\tilde{\mathbf{y}}, \quad (27)$$

$$\Sigma_2': \frac{d}{dt} \begin{bmatrix} \mathbf{z} \\ \tilde{\omega} \end{bmatrix} = \begin{bmatrix} \tilde{\omega} \\ -\xi(\mathbf{q}, \dot{\mathbf{q}}, \mathbf{z}, \tilde{\omega}) \end{bmatrix}. \quad (28)$$

It is easy to observe that the state space origin $[\tilde{\mathbf{y}}^T \ \mathbf{z}^T \ \tilde{\omega}^T]^T = \mathbf{0}$ is the unique equilibrium point. The stability of system (22) and (26) can be established by invoking Proposition 1.

Towards this end, it must be observed that the linear system Σ_1' : $(d/dt)\tilde{\mathbf{y}} = -K\tilde{\mathbf{y}}$ is GES; a suitable Lyapunov function is

$$V_1(\tilde{\mathbf{y}}) = \frac{1}{2}\tilde{\mathbf{y}}^T \tilde{\mathbf{y}}, \quad (29)$$

which trivially satisfies

$$c_1 \|\tilde{\mathbf{y}}\| \leq V_1(\tilde{\mathbf{y}}) \leq c_2 \|\tilde{\mathbf{y}}\|,$$

and

$$\left\| \frac{\partial V_1(\tilde{\mathbf{y}})}{\partial \tilde{\mathbf{y}}} \right\| \leq c_3 \|\tilde{\mathbf{y}}\|,$$

with $0 < c_1 < \frac{1}{2} < c_2$, and $1 < c_3$.

The time derivative along the trajectories of (27) yields

$$\dot{V}_1(\tilde{\mathbf{y}}) \leq -c_4 \|\tilde{\mathbf{y}}\|^2,$$

where $c_4 = \lambda_m\{K\}$. Thus, $V_1(\tilde{\mathbf{y}})$ holds the corresponding assumptions (11)–(14) globally.

On the other hand, in virtue of boundedness on the Jacobian (5), the disturbing term $J(\mathbf{q})\tilde{\omega}$ holds globally:

$$\|J(\mathbf{q})\tilde{\omega}\| \leq k_J \left\| \begin{bmatrix} \mathbf{z} \\ \tilde{\omega} \end{bmatrix} \right\|.$$

Therefore, the following stability result concerning the two-loops closed-loop system can be straightforwardly proven.

Proposition 2. Consider the resolved motion rate control (19) and the joint velocity control structure (23) and (24). Suppose that there exists a Lyapunov function $V_2(t, \mathbf{z}, \tilde{\omega})$ for system Σ_2' given in (28) such that

$$\begin{aligned} d_1 \left\| \begin{bmatrix} \mathbf{z} \\ \tilde{\omega} \end{bmatrix} \right\|^2 &\leq V_2(t, \mathbf{z}, \tilde{\omega}) \leq d_2 \left\| \begin{bmatrix} \mathbf{z} \\ \tilde{\omega} \end{bmatrix} \right\|^2, \\ \left\| \frac{\partial V_2(t, \mathbf{z}, \tilde{\omega})}{\partial \begin{bmatrix} \mathbf{z} \\ \tilde{\omega} \end{bmatrix}} \right\| &\leq d_3 \left\| \begin{bmatrix} \mathbf{z} \\ \tilde{\omega} \end{bmatrix} \right\|, \\ \dot{V}_2(t, \mathbf{z}, \tilde{\omega}) &\leq -d_4 \left\| \begin{bmatrix} \mathbf{z} \\ \tilde{\omega} \end{bmatrix} \right\|^2, \end{aligned} \quad (30)$$

for all $t \geq 0$, $\mathbf{z}, \tilde{\omega} \in \mathbb{R}^n$, and some positive constants d_1, d_2, d_3 , and d_4 . Then, the equilibrium point $[\tilde{\mathbf{y}}^T \ \mathbf{z}^T \ \tilde{\omega}^T]^T = \mathbf{0}$ of the closed-loop system (27) and (28) is GES.

Roughly speaking, Proposition 2 says that motion control of robot manipulators in operational space can be solved by using a two-loops control scheme where the outer loop corresponds to a kinematic control approach—resolved motion rate control—, and the inner loop to a joint velocity controller having a quite general structure (23), (24) provided that it is GES. This conclusion holds as long as the Jacobian $J(\mathbf{q})$ is nonsingular. In case the Jacobian is singular in a set of joint positions, then the desired end-effector pose \mathbf{y}_d must avoid such singular positions; the GES of the closed-loop system reduces to local exponential stability.

5. Model-based joint velocity controllers

In this section 2 model-based joint velocity controllers are analyzed. The stability of the overall closed-loop system, i.e. kinematic control (19) together with the joint velocity controllers, is established thanks to Proposition 2.

5.1. Velocity inner loop: inverse dynamics

A joint velocity controller based on inverse dynamics is given by

$$\tau = M(\mathbf{q})[\dot{\omega}_d + K_v \tilde{\omega} + K_i \mathbf{z}] + C(\mathbf{q}, \dot{\mathbf{q}})\dot{\mathbf{q}} + \mathbf{g}(\mathbf{q}), \quad (31)$$

$$\dot{\mathbf{z}} = \tilde{\omega}, \quad (32)$$

where $K_v, K_i \in \mathbb{R}^{n \times n}$ are symmetric positive definite matrices. Let us notice that the velocity controller (31), (32) is equivalent to controller (23), (24) with

$$\xi(\mathbf{q}, \dot{\mathbf{q}}, \mathbf{z}, \tilde{\omega}) = K_v \tilde{\omega} + K_i \mathbf{z}.$$

Hence, the system Σ'_2 given by (28) can be written as

$$\Sigma'_2: \frac{d}{dt} \begin{bmatrix} \mathbf{z} \\ \tilde{\omega} \end{bmatrix} = \begin{bmatrix} \tilde{\omega} \\ -K_v \tilde{\omega} - K_i \mathbf{z} \end{bmatrix}. \quad (33)$$

It is easy to observe that it is a linear system whose origin $[\mathbf{z}^T \tilde{\omega}^T]^T = \mathbf{0}$ is the unique equilibrium point.

5.1.1. Stability analysis

In order to prove GES of the closed-loop system, it remains to show that Σ'_2 satisfies condition (30) of Proposition 2. Towards this end, consider the Lyapunov function

$$V_2(\mathbf{z}, \tilde{\omega}) = \frac{1}{2}[\tilde{\omega} + \varepsilon \mathbf{z}]^T [\tilde{\omega} + \varepsilon \mathbf{z}] + \frac{1}{2} \mathbf{z}^T [K_i + \varepsilon K_v - \varepsilon^2 I] \mathbf{z}, \quad (34)$$

where ε holds

$$0 < \varepsilon < \lambda_m \{K_v\}. \quad (35)$$

Thus, $K_v - \varepsilon I > 0$ as well as $K_i + \varepsilon K_v - \varepsilon^2 I > 0$. The latter implies that $\lambda_m \{K_i + \varepsilon K_v - \varepsilon^2 I\} > 0$.

After some manipulations, it can be shown that

$$d_1 \left\| \begin{bmatrix} \mathbf{z} \\ \tilde{\omega} \end{bmatrix} \right\|^2 \leq V_2(\mathbf{z}, \tilde{\omega}) \leq d_2 \left\| \begin{bmatrix} \mathbf{z} \\ \tilde{\omega} \end{bmatrix} \right\|^2,$$

where

$$d_1 = \frac{1}{2} \lambda_m \left\{ \begin{bmatrix} \varepsilon^2 + \lambda_m \{K_i + \varepsilon K_v - \varepsilon^2 I\} & -\varepsilon \\ -\varepsilon & 1 \end{bmatrix} \right\} > 0,$$

and

$$d_2 = \frac{1}{2} \lambda_M \left\{ \begin{bmatrix} \varepsilon^2 + \lambda_M \{K_i + \varepsilon K_v - \varepsilon^2 I\} & \varepsilon \\ \varepsilon & 1 \end{bmatrix} \right\} > d_1.$$

On the other hand, the gradient of $V_2(\mathbf{z}, \tilde{\omega})$ yields

$$\left\| \frac{\partial V_2(\mathbf{z}, \tilde{\omega})}{\partial \begin{bmatrix} \mathbf{z} \\ \tilde{\omega} \end{bmatrix}} \right\| \leq d_3 \left\| \begin{bmatrix} \mathbf{z} \\ \tilde{\omega} \end{bmatrix} \right\|,$$

where

$$d_3 = \lambda_M \left\{ \begin{bmatrix} K_i + \varepsilon K_v & \varepsilon I \\ \varepsilon I & I \end{bmatrix} \right\} > 0.$$

Finally, the time derivative of $V_2(\mathbf{z}, \tilde{\omega})$ along the trajectories of system (33) is given by

$$\dot{V}_2(\mathbf{z}, \tilde{\omega}) = -\varepsilon \mathbf{z}^T K_i \mathbf{z} - \tilde{\omega}^T [K_v - \varepsilon I] \tilde{\omega} \leq -d_4 \left\| \begin{bmatrix} \mathbf{z} \\ \tilde{\omega} \end{bmatrix} \right\|^2,$$

where

$$d_4 = \lambda_m \left\{ \begin{bmatrix} \varepsilon K_i & 0 \\ 0 & K_v - \varepsilon I \end{bmatrix} \right\} > 0.$$

Hence, it has been shown that $V_2(\mathbf{z}, \tilde{\omega})$ satisfies the conditions (30) of Proposition 2. Then it is possible to claim that the control system formed by the resolved motion rate control (19) and the joint velocity controller (31), (32) leads to a GES closed-loop system.

5.2. Velocity inner loop: linear PI plus compensation

PI control is a classic strategy for velocity regulation in mechanisms. We propose the following extension of this technique for joint velocity control of robotic manipulators

$$\tau = K_v \tilde{\omega} + K_i \mathbf{z} + M(\mathbf{q})[\dot{\omega}_d + \Lambda \tilde{\omega}] + C(\mathbf{q}, \dot{\mathbf{q}})[\omega_d + \Lambda \mathbf{z}] + \mathbf{g}(\mathbf{q}), \quad (36)$$

$$\dot{\mathbf{z}} = \tilde{\omega}, \quad (37)$$

where $K_i, K_v \in \mathbb{R}^{n \times n}$ are symmetric positive definite matrices, and $\Lambda = K_v^{-1} K_i$. Control law (31) and (32) rely on the inverse dynamics philosophy. However, it does not possess a linear PI structure. In contrast, the control law (36) and (37) has a true linear PI term given by $K_v \tilde{\omega} + K_i \mathbf{z}$. Although the inverse dynamics approach may be more intuitive from a control design, the control law (36) and (37) has the advantage that it becomes the standard PI control plus acceleration feedforward when dealing with velocity tracking of linear actuators.

The controller (36) and (37) can be expressed as (23) and (24) with

$$\xi(\mathbf{q}, \dot{\mathbf{q}}, \mathbf{z}, \tilde{\omega}) = \Lambda \tilde{\omega} + M(\mathbf{q})^{-1} [C(\mathbf{q}, \dot{\mathbf{q}})[\tilde{\omega} + \Lambda \mathbf{z}] + K_v \tilde{\omega} + K_i \mathbf{z}].$$

With this choice, the system Σ'_2 given by (28) can be written as

$$\Sigma'_2: \frac{d}{dt} \begin{bmatrix} \mathbf{z} \\ \tilde{\omega} \end{bmatrix} = \begin{bmatrix} \tilde{\omega} \\ -M(\mathbf{q})^{-1} [C(\mathbf{q}, \dot{\mathbf{q}})[\tilde{\omega} + \Lambda \mathbf{z}] + K_v \dot{\tilde{\omega}} + K_i \mathbf{z}] + \Lambda \tilde{\omega} \end{bmatrix}. \quad (38)$$

This is a nonlinear and nonautonomous system whose unique equilibrium point is the origin of the state space $[\mathbf{z}^T \tilde{\omega}^T]^T = \mathbf{0}$.

5.2.1. Stability analysis

To carry out the stability analysis of (38), we propose the following Lyapunov function candidate inspired in [Spong, Ortega, and Kelly \(1990\)](#)

$$V_2(t, \mathbf{z}, \tilde{\omega}) = \frac{1}{2} [\tilde{\omega} + \Lambda \mathbf{z}]^T M(\mathbf{q}) [\tilde{\omega} + \Lambda \mathbf{z}] + \mathbf{z}^T K_i \mathbf{z}. \quad (39)$$

It can be shown that $V_2(t, z, \tilde{\omega})$ holds $V_2(t, \mathbf{0}, \mathbf{0}) = 0$ for all $t \geq 0$, and $V_2(t, z, \tilde{\omega}) > 0$ for all $t \geq 0$ and $[z^T \tilde{\omega}^T]^T \neq \mathbf{0}$. Hence, $V_2(t, z, \tilde{\omega})$ is a globally positive definite function. By this fact and noting that $V_2(t, z, \tilde{\omega})$ can be rewritten as

$$V_2(t, z, \tilde{\omega}) = \begin{bmatrix} z \\ \tilde{\omega} \end{bmatrix}^T P(q) \begin{bmatrix} z \\ \tilde{\omega} \end{bmatrix},$$

where

$$P(q) = \begin{bmatrix} K_i + A^T M(q) A & \frac{1}{2} A^T M(q) \\ \frac{1}{2} M(q) A & \frac{1}{2} M(q) \end{bmatrix},$$

it turns out that $P(q)$ is a positive definite matrix. This implies that

$$d_1 \left\| \begin{bmatrix} z \\ \tilde{\omega} \end{bmatrix} \right\|^2 \leq V_2(t, z, \tilde{\omega}) \leq d_2 \left\| \begin{bmatrix} z \\ \tilde{\omega} \end{bmatrix} \right\|^2$$

for all $t \geq 0$, and $z, \tilde{\omega} \in \mathbb{R}^n$, where

$$d_1 = \inf_{q \in \mathbb{R}^n} \lambda_m \{P(q)\} \quad \text{and} \quad d_2 = \sup_{q \in \mathbb{R}^n} \lambda_M \{P(q)\}.$$

It is worth noticing that the gradient of $V_2(t, z, \tilde{\omega})$ satisfies

$$\left\| \frac{\partial V_2(t, z, \tilde{\omega})}{\partial \begin{bmatrix} z \\ \tilde{\omega} \end{bmatrix}} \right\| \leq d_3 \left\| \begin{bmatrix} z \\ \tilde{\omega} \end{bmatrix} \right\|$$

with $d_3 = d_2$.

Evoking property (2), the time derivative $\dot{V}_2(t, z, \tilde{\omega})$ along the trajectories of (38) results

$$\dot{V}_2(t, z, \tilde{\omega}) = -z^T K_i K_v^{-1} K_i z - \tilde{\omega}^T K_v \tilde{\omega} \leq -d_4 \left\| \begin{bmatrix} z \\ \tilde{\omega} \end{bmatrix} \right\|^2,$$

where

$$d_4 = \lambda_m \left\{ \begin{bmatrix} K_i K_v^{-1} K_i & 0 \\ 0 & K_v \end{bmatrix} \right\} > 0.$$

At this point, it has been shown that $V_2(t, z, \tilde{\omega})$ satisfies condition (30) of Proposition 2—by the way, these conditions are sufficient to ensure that the joint velocity control system (38) is GES. More importantly, in virtue of Proposition 2 we have the conclusion that the control system obtained by utilizing the resolved motion rate control (19) together with the joint velocity controller (36) and (37) yields a GES closed-loop system.

6. Experimental results

A direct-drive arm with two vertical links has been designed and built at the CICESE Research Center—see Fig. 2. High torque, brushless direct-drive servos operating

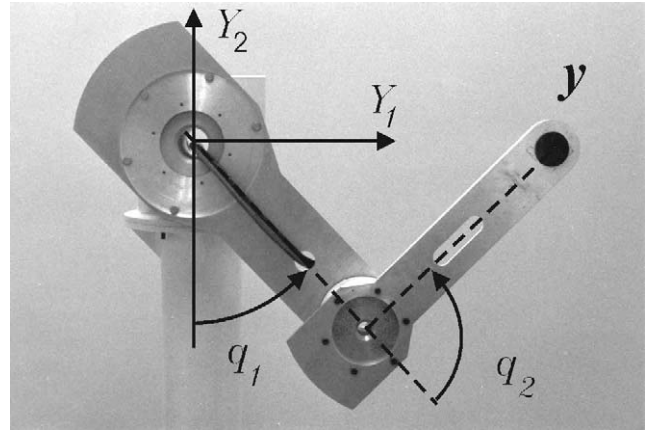


Fig. 2. Experimental arm.

in torque mode are used to drive the joints. A motion control board based on a TMS320C31 32-bit floating point microprocessor from Texas Instruments is used to execute the control algorithm. The control program is written in C programming language executed in the control board at 2.5 ms sampling period. The description of the experimental set-up is given in Reyes and Kelly (1997, 2001).

Experiments have shown that static and Coulomb friction at the motor joints are present and they depend in a complex manner on the joint positions and velocities. We have decided to compensate only viscous friction. The remaining friction types act as disturbances.

The experimental tests are concerned with the robot pose y meaning the Cartesian position of the arm tip—see Fig. 2. The direct kinematics is given by

$$h(q) = \begin{bmatrix} l_1 \sin(q_1) + l_2 \sin(q_1 + q_2) \\ -l_2 \cos(q_1) - l_2 \cos(q_1 + q_2) \end{bmatrix},$$

where l_1 and l_2 are the link lengths. Thus, the Jacobian matrix results

$$J(q) = \begin{bmatrix} l_1 \cos(q_1) + l_2 \cos(q_1 + q_2) & l_2 \cos(q_1 + q_2) \\ l_2 \sin(q_1) + l_2 \sin(q_1 + q_2) & l_2 \sin(q_1 + q_2) \end{bmatrix}.$$

The desired trajectory chosen for the experimental evaluation was

$$y_d(t) = \begin{bmatrix} y_{1c} + a \cos(\omega t - \phi) \\ y_{2c} + a \sin(\omega t - \phi) \end{bmatrix}, \quad (40)$$

where $y_{1c} = y_{2c} = 0.318$ m, $a = 0.2$ m, $\omega = 0.5$ rad/s and $\phi = 0.7$ rad. This trajectory makes the arm tip trace a circle in the plane y_1 – y_2 having a radius $a = 0.2$ m.

All experimental tests were carried out under the initial condition $q_1(0) = 45^\circ$, $q_2(0) = 90^\circ$, and $\dot{q}_1(0) = \dot{q}_2(0) = 0^\circ/\text{s}$.

6.1. Inverse kinematics plus computed-torque control

For comparison purpose, first a classic control approach was utilized to solve the motion control problem in operational space. To this end, the desired trajectory $y_d(t)$ in (40)

was translated to the corresponding joint space desired position trajectory $\mathbf{q}_d(t)$ via the inverse kinematics of the experimental two degrees-of-freedom arm:

$$\mathbf{q}_d = \mathbf{h}^{-1}(\mathbf{y}_d) = \begin{bmatrix} \frac{\pi}{2} + \tan^{-1}\left(\frac{y_{d2}}{y_{d1}}\right) - \tan^{-1}\left(\frac{l_2 \sin(q_{d2})}{l_1 + l_2 \cos(q_{d2})}\right), \\ \cos^{-1}\left(\frac{y_{d1}^2 + y_{d2}^2 - l_1^2 - l_2^2}{2l_1 l_2}\right) \end{bmatrix}, \quad (41)$$

where $\mathbf{h}^{-1}(\mathbf{y}_d)$ denotes the inverse kinematics as function of the desired operational space trajectory \mathbf{y}_d in (40). Additionally, the desired joint velocity and acceleration, are given by

$$\dot{\mathbf{q}}_d = \mathbf{J}(\mathbf{q}_d)^{-1} \begin{bmatrix} \dot{y}_{d1} \\ \dot{y}_{d2} \end{bmatrix},$$

$$\ddot{\mathbf{q}}_d = \left[\frac{d}{dt} \mathbf{J}(\mathbf{q}_d)^{-1} \right] \begin{bmatrix} \dot{y}_{d1} \\ \dot{y}_{d2} \end{bmatrix} + \mathbf{J}(\mathbf{q}_d)^{-1} \begin{bmatrix} \ddot{y}_{d1} \\ \ddot{y}_{d2} \end{bmatrix},$$

which result is valid because \mathbf{y}_d remains away from singular configurations.

Once the desired joint trajectory $\mathbf{q}_d(t)$ is available, then a trajectory tracking controller in joint space can be evoked. We have considered the computed-torque control algorithm given by Spong and Vidyasagar (1989), Sciavicco and Siciliano (2000),

$$\boldsymbol{\tau} = \mathbf{M}(\mathbf{q})\mathbf{u}_0 + \mathbf{C}(\mathbf{q}, \dot{\mathbf{q}})\dot{\mathbf{q}} + \mathbf{g}(\mathbf{q}), \quad (42)$$

where

$$\mathbf{u}_0 = \ddot{\mathbf{q}}_d + \mathbf{K}_v[\dot{\mathbf{q}}_d - \dot{\mathbf{q}}] + \mathbf{K}_p[\mathbf{q}_d - \mathbf{q}] \quad (43)$$

with $\mathbf{K}_v, \mathbf{K}_p \in \mathbb{R}^{2 \times 2}$ symmetric positive definite matrices. It can be shown that this controller yields a GES closed-loop system, thus

$$\lim_{t \rightarrow \infty} [\mathbf{h}^{-1}(\mathbf{y}_d(t)) - \mathbf{q}(t)] = \mathbf{0}$$

is attained which means that the desired motion in joint and operational spaces are accomplished.

We have conducted an experiment to test the joint space based trajectory tracking controller (42) and (43) with the desired joint space trajectory (41). The controller gains \mathbf{K}_p and \mathbf{K}_v were selected as $\mathbf{K}_p = \text{diag}\{1000, 1000\} 1/s^2$, $\mathbf{K}_v = \text{diag}\{63.24, 63.24\} 1/s$, which were chosen to avoid torque saturation at the beginning of the test. The experimental results are shown in Figs. 3 and 4, where the operational space tracking errors— \tilde{y}_1 and \tilde{y}_2 —, and the applied torques, are depicted. Notwithstanding, steady-state tracking error peaks are observed in Fig. 3. These peaks coincide with the change of sign of the joint velocity, so they are attributed to uncompensated Coulomb friction. The maximum observed peak is 0.875 cm for \tilde{y}_1 and 0.75 cm for \tilde{y}_2 . Thus, the relative error with respect to the circle's radius ($a = 20$ cm) is 4.38%, and 3.75%. The applied torques τ_1 and τ_2 depicted in Fig. 4 remain in the safety below the saturation limits (150 and 15 Nm, respectively).

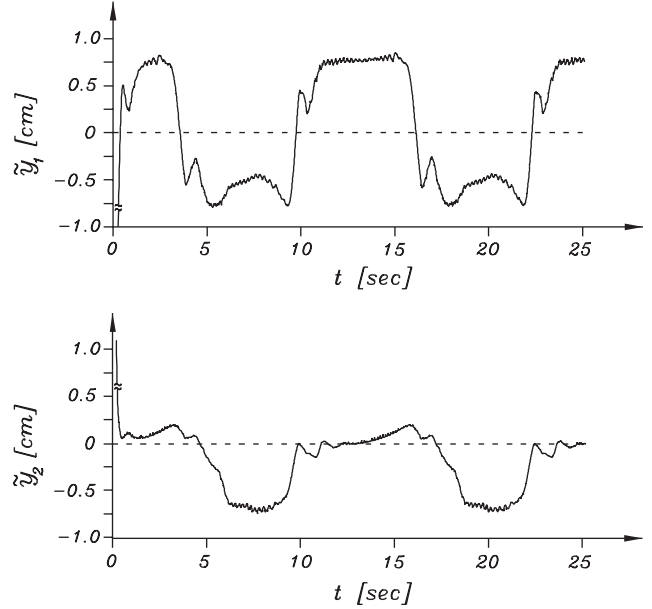


Fig. 3. Tracking errors: Computed-torque control.

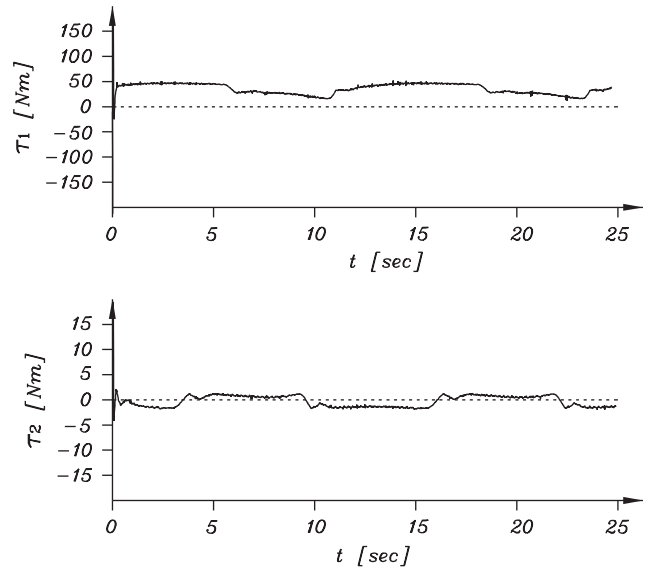


Fig. 4. Input torques: Computed-torque control.

6.2. Velocity inner loop: Inverse dynamics

Experiments were carried out using the two-loops control scheme composed by the resolved motion rate control (19) together with the inverse dynamics-based velocity controller (31), (32). The controller gains were chosen as $\mathbf{K} = \text{diag}\{5, 5\} 1/s$, $\mathbf{K}_i = \text{diag}\{1000, 5000\} 1/s^2$, $\mathbf{K}_v = \text{diag}\{63.25, 141.42\} 1/s$.

Similar to the computed-torque control (42) and (43), the controller gains were chosen in order to avoid torque saturation at the beginning of the test. In Fig. 5 the trajectory tracking errors \tilde{y}_1 and \tilde{y}_2 are shown. The largest tracking

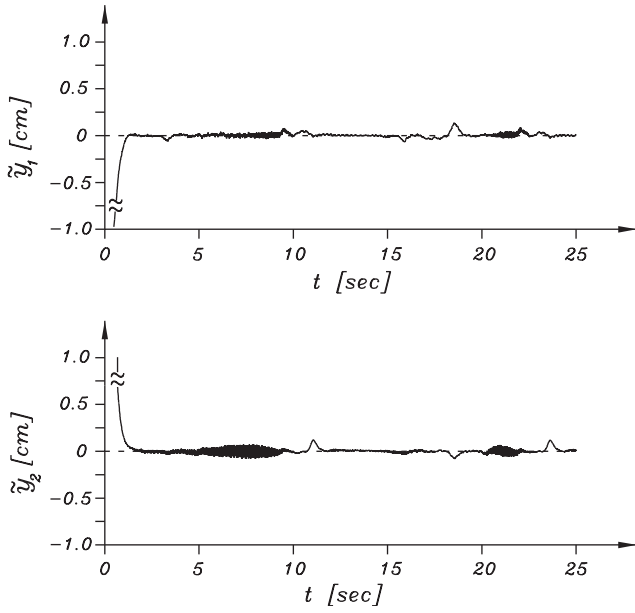


Fig. 5. Tracking errors: Kinematic control plus inverse dynamics-based joint velocity controller.

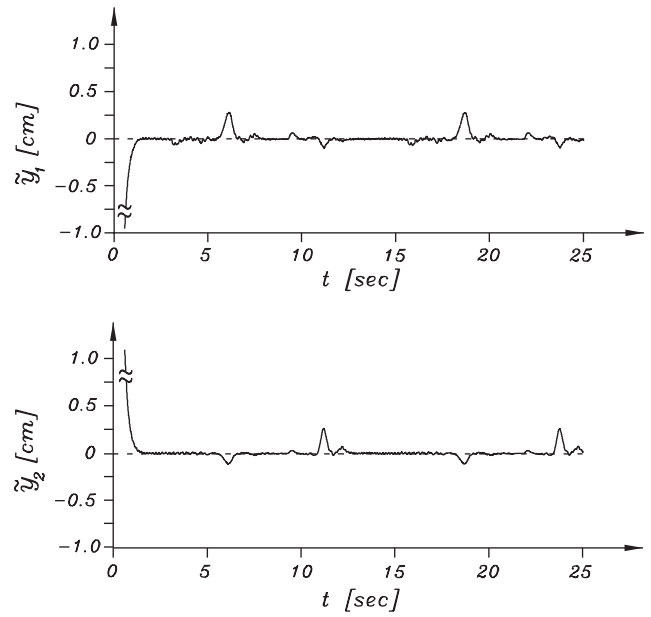


Fig. 7. Tracking errors: Kinematic control plus PI with compensation joint velocity controller.

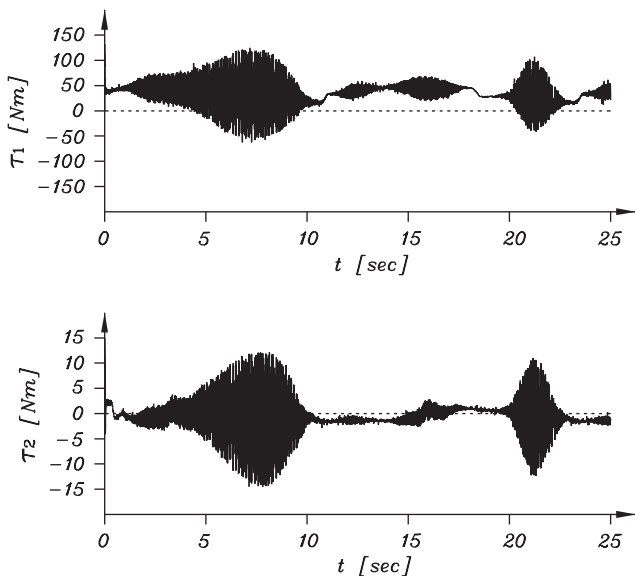


Fig. 6. Input torques: Kinematic control plus inverse dynamics-based joint velocity controller.

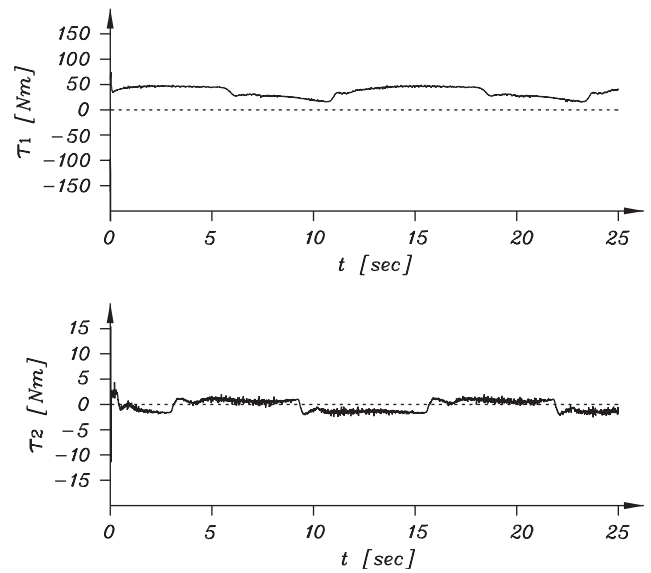


Fig. 8. Input torques: Kinematic control plus PI with compensation joint velocity controller.

error peak were 0.13 cm for \tilde{y}_1 and 0.11 cm for \tilde{y}_2 . With respect to circle's radius ($a = 20$ cm) of the desired trajectory \mathbf{y}_d , they represent deviation errors of 0.67% and 0.59%, respectively. The performance is meaningfully better than the joint space controller (42) and (43). Nevertheless, Fig. 6 shows that the applied torques present high-frequency oscillations. They are occasioned by the joint velocity estimation via Euler approximation, but they can be reduced with smaller control gains.

6.3. Velocity inner loop: Linear PI plus compensation

The third experiment was developed using the PI plus compensation joint velocity controller (36), (37) as inner loop. The controller gains were chosen as $K = \text{diag}\{5, 5\} \text{ 1/s}$, $K_i = \text{diag}\{1000, 1000\} \text{ Nm/rad}$, $K_v = \text{diag}\{63.25, 15.0\} \text{ Nm s/rad}$.

Fig. 7 shows the time evolution of tracking errors \tilde{y}_1 and \tilde{y}_2 ; Fig. 8 depicts the applied torques. The larger tracking error peak was 0.3 cm for \tilde{y}_1 and 0.256 cm for \tilde{y}_2 ; this gives

deviation errors of 1.5% and 1.28% with respect to circle's radius of the desired trajectory y_d , respectively. On the other hand, the applied torques τ_1 and τ_2 shown in Fig. 8 have a smoother behavior than the inverse dynamics velocity control scheme.

In view of the presented results, it is clear that the two control schemes designed on the two-loops strategy behave similar; the performance is much better than the approach based on the inverse kinematics resolution together with the computed-torque control technique. The main reason for this result is that the closure of the outer loop improves the robustness of the two-loops control scheme with respect to the single-loop control system.

7. Concluding remarks

This paper has studied control systems based on two-loops structure for motion control of robot manipulators in operational space. The outer loop corresponds to a kinematic control structure (resolved motion rate control), and the inner loop to a general joint velocity control scheme has been proposed. It is shown that the overall closed-loop system can be seen as a cascade system. Using tools of such a field, a particular stability result has been presented. Roughly speaking, it states that if the joint velocity inner loop is GES, then the complete closed-loop system is also GES. This theoretical result explains why most of industrial robots, which have low level inner joint velocity regulators, are effectively controlled in operational space by adding outer loops (kinematics control). Experiments have been conducted on a two degrees-of-freedom direct-drive arm. For the same operational space desired motion task, experimental comparisons between the computed-torque control and the proposed two-loops controllers (kinematic control plus joint velocity inner loop control) were presented. The best performances were achieved using the latter two-loops control schemes.

References

- Aicardi, M., Caiti, A., Cannata, G., & Casalino, G. (1995). Stability and robustness of a two layered hierarchical architecture for the closed loop control of robots in the operational space. In *Proceedings of the IEEE international conference on robotics and automation* (pp. 2771–2778). Nagoya, Japan.
- Canudas, C., Siciliano, B., & Bastin, G. (Eds). (1996). *Theory of robot control*. London: Springer.
- Corke, P. (1994). *The unimation puma servo system*. Report MTM-226, CSIRO Division of Manufacturing Technology, Australia, July.
- Hsu, P., Hauser, J., & Sastry, S. S. (1989). Dynamic control of redundant manipulators. *Journal of Robotic Systems*, 6, 133–148.
- Isidori, A. (1999). *Nonlinear control systems II*. London: Springer.
- Khalil, H. (1996). *Nonlinear systems*. Upper-Saddle River: Prentice-Hall.
- Loria, A., Fossen, T. I., & Panteley, E. (2000). A separation principle for dynamic positioning of ships: Theoretical and experimental results. *IEEE Transactions on Control Systems Technology*, 8(2), 332–343.
- Nilsson, K. (1996). *Industrial robot programming*. Ph.D. thesis, Lund Institute of Technology, Department of Automatic Control, Sweden.
- Panteley, E., & Loria, A. (1998). On global uniform asymptotic stability of nonlinear time-varying systems in cascade. *Systems and Control Letters*, 33, 131–138.
- Panteley, E., Loria, A., & Sokolov, A. (1999). Global uniform asymptotic stability of cascaded non autonomous nonlinear systems: Application to stabilization of a diesel engine. *European Journal of Control*, 5, 107–115.
- Reyes, F., & Kelly, R. (1997). Evaluation of identification schemes on a direct drive robot. *Robotica*, 15, 563–571.
- Reyes, F., & Kelly, R. (2001). Experimental evaluation of model-based controllers on a direct-drive robot arm. *Mechatronics*, 11, 267–282.
- Sciavicco, L., & Siciliano, B. (2000). *Modeling and control of robot manipulators*. London: Springer.
- Sepulchre, R., Janković, M., & Kokotović, P. (1997). *Constructive nonlinear control*. London: Springer.
- Slotine, J. J., & Li, W. (1991). *Applied nonlinear control*. Englewood Cliffs: Prentice-Hall.
- Spong, M., Ortega, R., & Kelly, R. (1990). Comments on “Adaptive manipulator control: A case study”. *IEEE Transactions on Automatic Control*, 35(6), 761–762.
- Spong, M. W., & Vidyasagar, M. (1989). *Robot dynamics and control*. New York: Wiley.
- Vidyasagar, M. (1993). *Nonlinear systems analysis*. Englewood Cliffs: Prentice-Hall.
- Wampler, C. W., & Leifer, L. J. (1988). Applications of damped least-squares methods to resolved-rate and resolved-acceleration control of manipulators. *ASME Journal of Dynamic Systems, Measurement, and Control*, 110, 31–38.
- Whitney, D. E. (1969). Resolved motion rate control of manipulators and human prostheses. *IEEE Transactions on Man Machine Systems*, MMS-10(2), 47–53.



Rafael Kelly was born in Monterrey, Mexico, in 1959. He received the B.S. degree in physics from the Instituto Tecnológico y de Estudios Superiores de Monterrey, Mexico, and the Ph.D. degree in automatic control from the Institut National Polytechnique de Grenoble, France, in 1980 and 1986, respectively. He is currently a Professor at the Centro de Investigación Científica y de Educación Superior de Ensenada, Mexico. His research interests include robotics, automatic control and information technologies.



Javier Moreno was born in Culiacán, Mexico, in 1974. He received the B.Sc. degree in Electronics Engineering from the Instituto Tecnológico de Culiacán, Mexico, in 1997, and the Ph.D. degree in Automatic Control from the Centro de Investigación Científica y de Educación Superior de Ensenada, CI-CESE, Mexico, in 2002. He was an Associate Researcher at the Centro de Investigación y Desarrollo de Tecnología Digital del IPN, CITEDI-IPN, Tijuana, Mexico, from 2002 to 2004. Currently, he is a Postdoctoral Fellow at the Université de Liège, Belgium. His main research interests are control of electro-mechanical systems.